Unique steady annual cycle in marine ecosystem model simulations

Markus Pfeil[1] and Thomas Slawig[1]

[1]Kiel Marine Science (KMS) - Centre for Interdisciplinary Marine Science, Dep. of Computer Science, Kiel University, 24098 Kiel, Germany ({mpf, ts}@informatik.uni-kiel.de).

arXiv:2111.15424v1 [q-bio.PE] 30 Nov 2021

Abstract

Marine ecosystem models are an important tool to assess the role of the ocean biota in climate change and to identify relevant biogeochemical processes by validating the model outputs against observational data. For the assessment of the marine ecosystem models, the existence and uniqueness of an annual periodic solution (i.e., a steady annual cycle) is desirable. To analyze the uniqueness of a steady annual cycle, we performed a larger number of simulations starting from different initial concentrations for a hierarchy of biogeochemical models with an increasing complexity. The numerical results suggested that the simulations finished always with the same steady annual cycle regardless of the initial concentration. Due to numerical instabilities, some inadmissible approximations of the steady annual cycle, however, occurred in some cases for the three most complex biogeochemical models. Our numerical results indicate a unique steady annual cycle for practical applications.

1 Introduction

In the field of climate research, marine ecosystem models are an important tool to assess the role of marine biogeochemical processes in climate change. These models are generally an essential component for the analysis of biogeochemical processes influencing the marine ecosystem. As part of the global carbon cycle, the ocean, specifically, takes up CO_2 from the atmosphere and stores it and, subsequently, the marine carbon affects the ocean biota. In addition to the biogeochemical processes, a marine ecosystem model takes into account the physical processes as well as the interplay between the physical and biogeochemical processes wherefore a marine ecosystem model consists of a global circulation model coupled to a biogeochemical model (cf. Fasham 2003; Sarmiento and Gruber 2006; W. Fennel and Neumann 2004). The physical processes describing the ocean circulation are well known to include the equations and variables. Conversely, there is generally no set of equations and variables describing the biogeochemical processes. Therefore, many different biogeochemical models with varying complexity exist which differ in the number of state variables and parametrizations (e.g., Kriest, Khatiwala, and Oschlies 2010; Keller, Oschlies, and Eby 2012; Ilyina et al. 2013; Yool, Popova,

and Anderson 2013; Le Quéré et al. 2016). For these different biogeochemical models, validation and assessment is necessary to evaluate the simulated steady annual cycle against observational data (cf. K. Fennel et al. 2001; Schartau and Oschlies 2003). This requires a parameter optimization and a discussion of simulation results for each biogeochemical model.

The biogeochemical model assessment is based on the existence and uniqueness of periodic solutions. If different periodic solutions exist for one model parameter vector, parameter optimizations or sensitivity studies are practically impossible. Furthermore, the interpretation of numerically obtained steady annual cycles is difficult if a non periodic solution of the continuous equations exists. Therefore, theoretical results about the existence and uniqueness of periodic solutions are helpful and desired to validate the numerical results. However, the theoretical analysis is a challenging task so far without a proof for a unique periodic annual cycle for complex biogeochemical models (Roschat and Slawig 2014; Roschat and Slawig 2015). In this paper, we analyzed the uniqueness of a steady annual cycle by running a larger number of simulations starting from different initial concentrations for a hierarchy of biogeochemical models with an increasing complexity. In addition to the mostly used constant initial concentration, we applied a wide variety of randomly generated initial concentrations for the different biogeochemical models. A unique steady annual cycle in these numerical simulations is, indeed, an indication for practical applications but it does not in general allow any conclusion about the existence and uniqueness of periodic solutions.

The paper is organized as follows: next, we describe marine ecosystem models including the computation of steady annual cycles (Section 2). In Section 3, we present a wide variety of different initial concentrations. Numerical results of the steady annual cycle computation starting from different initial concentrations are discussed in Section 4. The paper closes with a summary and conclusions (Section 5).

2 Model description

A marine ecosystem model describes the interplay of the ocean circulation and the marine biogeochemical processes. The modeling of the marine ecosystem comprises a given number of ecosystem species (or biogeochemical tracers), which are substances in marine water and part of the biogeochemical cycle (i.e., subject to chemical and biochemical reactions). In a fully coupled marine ecosystem model (also called *online* model), the ocean circulation affects the biogeochemical tracers and, vice versa, the biogeochemical tracers influence the ocean circulation. Due to the full coupling, a simulation using such a model is computationally expensive and, therefore, generally limited to single model evaluations because a computation of a steady annual cycle requires a long-time integration over several millennia (Oschlies 2006; Bernsen, Dijkstra, and Wubs 2008; Bryan 1984; Danabasoglu, McWilliams, and Large 1996). In contrast to an online model, an *offline* model neglects the influence of the biogeochemical tracers on the ocean circulation. As a result, this one-way coupling enables the application of a pre-computed ocean circulation and reduces the computational effort. In this paper, we approximated marine

ecosystem models using an offline model with an increasing complexity of the biogeochemical models introduced by Kriest, Khatiwala, and Oschlies (2010) and Dutkiewicz et al. (2005).

2.1 Model equations for marine ecosystems

A system of partial differential equations represents the marine ecosystem model. The number of modeled tracers determines the complexity of the marine ecosystem model and, thus, the size of the system of differential equations. In the rest of this paper, we consider marine ecosystem models using an offline model with $n_y \in \mathbb{N}$ tracers on a spatial domain $\Omega \subset \mathbb{R}^3$ (i.e., the ocean) and a time interval $[0,1]$ (i.e., one model year). Function $y_i : \Omega \times [0,1] \to \mathbb{R}$, $i \in \{1,\dots,n_y\}$, describes the tracer concentrations of tracer y_i and $\mathbf{y} := (y_i)_{i=1}^{n_y}$ summarizes the tracer concentrations of all tracers. For $i = 1,\dots,n_y$, the system of parabolic partial differential equations

$$\frac{\partial y_i}{\partial t}(x,t) + (D(x,t) + A(x,t))\, y_i(x,t) = q_i\left(x,t,\mathbf{y},\mathbf{u}\right), \qquad x \in \Omega, t \in [0,1], \quad (1)$$

$$\frac{\partial y_i}{\partial n}(x,t) = 0, \qquad x \in \partial\Omega, t \in [0,1], \quad (2)$$

describes the tracer transport of a marine ecosystem model. Here, the homogeneous Neumann boundary condition (2) includes the normal derivative and models no fluxes on the boundary.

The ocean currents, modeled by spatially discretized advection and diffusion, transport the tracers in marine water. The linear operator $A : \Omega \times [0,1] \to \mathbb{R}$ describes the advection as

$$A(x,t)y_i(x,t) := \operatorname{div}\left(v(x,t)y_i(x,t)\right), \qquad x \in \Omega, t \in [0,1], \quad (3)$$

$i \in \{1,\dots,n_y\}$, using a given velocity field $v : \Omega \times [0,1] \to \mathbb{R}^3$. The diffusion operator $D : \Omega \times [0,1] \to \mathbb{R}$ models the turbulent effects of the ocean circulation but neglects the molecular diffusion of the tracers themselves because this is known to be much smaller than the diffusion induced by turbulence. Due to the quite different spatial scales in horizontal and vertical direction, the diffusion operator requires a splitting $D = D_h + D_v$ into a horizontal and a vertical part and an implicit treatment of the vertical part D_v in the time-integration. Both directions are modeled in the second-order form as

$$D_h(x,t)y_i(x,t) := -\operatorname{div}_h\left(\kappa_h(x,t)\nabla_h y_i(x,t)\right) \qquad x \in \Omega, t \in [0,1], \quad (4)$$

$$D_v(x,t)y_i(x,t) := -\frac{\partial}{\partial z}\left(\kappa_v(x,t)\frac{\partial y_i}{\partial z}(x,t)\right), \qquad x \in \Omega, t \in [0,1], \quad (5)$$

$i \in \{1,\dots,n_y\}$, where div_h and ∇_h denote the horizontal divergence and gradient, $\kappa_h, \kappa_v : \Omega \times [0,1] \to \mathbb{R}$ the diffusion coefficient fields and z the vertical coordinate. The diffusion coefficient fields are identical for all tracers since the molecular diffusion is neglected.

The biogeochemical model contains the biogeochemical processes modeled in the marine ecosystem. In addition to the biogeochemical model, the marine ecosystem model

also takes the effects of the ocean dynamics into account and, therefore, contains the whole system (1) to (6). The nonlinear function $q_i : \Omega \times [0,1] \to \mathbb{R}, (x,t) \mapsto q_i(x,t,\mathbf{y},\mathbf{u})$ represents the biogeochemical processes for tracer y_i, $i \in \{1,\dots,n_y\}$. Indeed, these functions q_i depend, firstly, on space and time (for example, on the variability of the solar radiation), secondly, on the coupling to the other tracers and, thirdly, on $n_u \in \mathbb{R}$ model parameters $\mathbf{u} \in \mathbb{R}^{n_u}$ (such as growth, loss and mortality rates or sinking speed). The biogeochemical model $\mathbf{q} = (q_i)_{i=1}^{n_y}$ summarizes the biogeochemical processes of all tracers.

An annually periodic solution of the marine ecosystem model (i.e., a steady annual cycle) fulfills in addition to (1) and (2)

$$y_i(x,0) = y_i(x,1), \qquad x \in \Omega, \tag{6}$$

for $i = 1,\dots,n_y$. Therefore, we assume that the operators A, D and the functions q_i are also annually periodic in time.

2.2 Biogeochemical models

The biogeochemical models differ in the given number of ecosystem species. In the present paper, we applied a hierarchy of five different biogeochemical models with an increasing complexity introduced by Kriest, Khatiwala, and Oschlies (2010) as well as a biogeochemical model introduced by Dutkiewicz et al. (2005). In the following, we briefly introduce the biogeochemical models but we refer to Kriest, Khatiwala, and Oschlies (2010), Dutkiewicz et al. (2005), and Piwonski and Slawig (2016) for a detailed description of the modeled processes and model equations. Table 1 summarizes the model parameters of the biogeochemical models. Moreover, Table 2 contains the assignment of the model parameters to the various biogeochemical models and the values used in this paper.

Many biogeochemical processes depend on the amount of available light. Based on the astronomical formula of Paltridge and Platt (1976) and taking into account the ice cover, the exponential attenuation of water as well as phytoplankton (if included in the model), the light intensity is described by the light limitation function $I : \Omega \times [0,1] \to \mathbb{R}_{\geq 0}$. Due to the decreasing light intensity, the ocean is divided into a euphotic (sun lit) zone of about 100 m and an aphotic zone below. The biological production (for example, photosynthesis, grazing or mortality) takes place mainly in the euphotic zone, and particulate matter sinks to depth where it remineralizes according to the empirical law relationship (Martin et al. 1987).

The N model contains only one tracer modeling phosphate (PO_4) as inorganic nutrients (N) (i.e., $\mathbf{y} = \mathbf{y}_{\mathrm{N}}$) and is the simplest biochemical model of the hierarchy (cf. Bacastow and Maier-Reimer 1990; Kriest, Khatiwala, and Oschlies 2010). Depending on available nutrients and light, the phytoplankton production (or biological uptake)

$$f_P : \Omega \times [0,1] \to \mathbb{R}, f_P(x,t) = \mu_P y_P^* \frac{I(x,t)}{K_I + I(x,t)} \frac{\mathbf{y}_N(x,t)}{K_N + \mathbf{y}_N(x,t)} \tag{7}$$

Table 1: Model parameters of the biogeochemical models.

Parameter	Description	Unit
k_w	Attenuation coefficient of water	m^{-1}
k_c	Attenuation coefficient of phytoplankton	$(\,\mathrm{mmol\,P\,m^{-3}}\,)^{-1}\,\mathrm{m}^{-1}$
μ_P	Maximum growth rate	d^{-1}
μ_Z	Maximum grazing rate	d^{-1}
K_N	Half saturation constant for PO_4 uptake	$\mathrm{mmol\,P\,m^{-3}}$
K_P	Half saturation constant for grazing	$\mathrm{mmol\,P\,m^{-3}}$
K_I	Light intensity compensation	$\mathrm{W\,m^{-2}}$
σ_Z	Fraction of production remaining in Z	1
σ_{DOP}	Fraction of losses assigned to DOP	1
λ_P	Linear phytoplankton loss rate	d^{-1}
κ_P	Quadratic phytoplankton loss rate	$(\,\mathrm{mmol\,P\,m^{-3}}\,)^{-1}\,\mathrm{d}^{-1}$
λ_Z	Linear zooplankton loss rate	d^{-1}
κ_Z	Quadratic zooplankton loss rate	$(\,\mathrm{mmol\,P\,m^{-3}}\,)^{-1}\,\mathrm{d}^{-1}$
k_c	Attenuation coefficient of phytoplankton	$(\,\mathrm{mmol\,P\,m^{-3}}\,)^{-1}\,\mathrm{d}^{-1}$
λ'_P	Phytoplankton mortality rate	d^{-1}
λ'_Z	Zooplankton mortality rate	d^{-1}
λ'_D	Degradation rate	d^{-1}
λ'_{DOP}	Decay rate	yr^{-1}
b	Implicit representation of sinking speed	1
a_D	Depth-dependent increase of sinking speed	d^{-1}
b_D	Initial sinking speed	$\mathrm{m\,d}^{-1}$

is limited by a maximum production rate $\mu_P \in \mathbb{R}_{>0}$ and applies an implicitly prescribed concentration of phytoplankton $y_P^* = 0.0028\ \mathrm{mmol\,P\,m^{-3}}$. Table 2 lists the $n_u = 5$ model parameters.

The N-DOP model includes two tracers, nutrients (N) and dissolved organic phosphorus (DOP), i.e. $\mathbf{y} = (\mathbf{y}_{\mathrm{N}}, \mathbf{y}_{\mathrm{DOP}})$ (cf. Bacastow and Maier-Reimer 1991; Parekh, Follows, and Boyle 2005; Kriest, Khatiwala, and Oschlies 2010). Using the same phytoplankton production (7) as the N model, the N-DOP contains $n_u = 7$ model parameters (see Table 2).

The NP-DOP model comprises three tracers: nutrients (N), phytoplankton (P) and dissolved organic phosphorus (DOP), i.e., $\mathbf{y} = (\mathbf{y}_{\mathrm{N}}, \mathbf{y}_{\mathrm{P}}, \mathbf{y}_{\mathrm{DOP}})$ (cf. Kriest, Khatiwala, and Oschlies 2010). Instead of using an implicit treatment y_P^* of phytoplankton, the NP-DOP model computes the phytoplankton production (7) using the explicit phytoplankton concentration $\mathbf{y}_{\mathrm{P}}$. Using the implicitly prescribed zooplankton concentration $y_Z^* = 0.01\ \mathrm{mmol\,P\,m^{-3}}$, the zooplankton grazing

$$f_Z : \Omega \times [0,1] \to \mathbb{R}, f_Z(x,t) = \mu_Z y_Z^* \frac{\mathbf{y}_P(x,t)^2}{K_P^2 + \mathbf{y}_P(x,t)^2} \tag{8}$$

models the loss of phytoplankton. Overall, this model includes the $n_u = 13$ model

Table 2: Assignment of the model parameters to the biogeochemical models and used parameter values. The model parameters of the MITgcm-PO4-DOP model correspond to those of the N-DOP model.

Parameter	N	N-DOP	NP-DOP	NPZ-DOP	NPZD-DOP
k_w	0.02	0.02	0.02	0.02	0.02
k_c			0.48	0.48	0.48
μ_P	2.0	2.0	2.0	2.0	2.0
μ_Z			2.0	2.0	2.0
K_N	0.5	0.5	0.5	0.5	0.5
K_P			0.088	0.088	0.088
K_I	30.0	30.0	30.0	30.0	30.0
σ_Z				0.75	0.75
σ_{DOP}		0.67	0.67	0.67	0.67
λ_P			0.04	0.04	0.04
κ_P			4.0		
λ_Z				0.03	0.03
κ_Z				3.2	3.2
λ'_P			0.01	0.01	0.01
λ'_Z				0.01	0.01
λ'_D					0.05
λ'_{DOP}		0.5	0.5	0.5	0.5
b	0.858	0.858	0.858	0.858	
a_D					0.058
b_D					0.0

parameters listed in Table 2.

The NPZ-DOP model includes four tracers, nutrients (N), phytoplankton (P), zooplankton (Z) and dissolved organic phosphorus (DOP), i.e., $\mathbf{y} = (\mathbf{y}_{\mathrm{N}}, \mathbf{y}_{\mathrm{P}}, \mathbf{y}_{\mathrm{Z}}, \mathbf{y}_{\mathrm{DOP}})$ (cf. Kriest, Khatiwala, and Oschlies 2010). The phytoplankton production (7) and zooplankton grazing (8) are the same as for the NP-DOP model but this model uses explicitly the zooplankton concentration $\mathbf{y}_{\mathrm{Z}}$ instead of implicitly prescribed concentration y^*_Z. Table 2 lists the $n_u = 16$ model parameters.

The NPZD-DOP model comprises five tracers, nutrients (N), phytoplankton (P), zooplankton (Z), detritus (D) and dissolved organic phosphorus (DOP), i.e., $\mathbf{y} = (\mathbf{y}_{\mathrm{N}}, \mathbf{y}_{\mathrm{P}}, \mathbf{y}_{\mathrm{Z}}, \mathbf{y}_{\mathrm{D}}, \mathbf{y}_{\mathrm{DOP}})$, and is the most complex biogeochemical model of the hierarchy (cf. Schmittner et al. 2005; Kriest, Khatiwala, and Oschlies 2010). Using the phytoplankton production (7) and zooplankton grazing (8) as for the NPZ-DOP model, the NPZD-DOP contains $n_u = 18$ model parameters (see Table 2).

The MITgcm-PO4-DOP model contains two tracers, phosphate (PO_4) and dissolved organic phosphorus (DOP), i.e. $\mathbf{y} = (\mathbf{y}_{\mathrm{N}}, \mathbf{y}_{\mathrm{DOP}})$ (cf. Dutkiewicz et al. 2005). This model resembles the N-DOP model and, therefore, we identified the $n_u = 7$ model parameters with those of the N-DOP model (see Table 2).

2.3 Transport matrix method

The *transport matrix method* (TMM) efficiently approximates the tracer transport of the ocean circulation by matrix-vector multiplications (Khatiwala, Visbeck, and Cane 2005; Khatiwala 2007). The discretized advection-diffusion equation can be written as a linear matrix equation because the application of the advection and diffusion operator, A and D, on a spatially discretized tracer vector is linear. Therefore, the TMM replaces the direct implementation of a discretization scheme for the advection and diffusion by the application of matrices approximating the ocean circulation. In particular, the TMM approximates the ocean circulation only with these matrices including the influence of all parameterized processes represented in the underlying ocean circulation model on the transport (Khatiwala, Visbeck, and Cane 2005).

Using the TMM, each time step of the simulation for a marine ecosystem model consists only of two matrix-vector multiplications, modeling the ocean circulation, and an evaluation of the biogeochemical model. In order to discretize the advection-diffusion equation, we use a grid with $n_x \in \mathbb{N}$ grid points $(x_k)_{k=1}^{n_x}$ as spatial discretization of the domain Ω (i.e., the ocean) and the time steps $t_0, \ldots, t_{n_t} \in [0,1]$, $n_t \in \mathbb{N}$, specified by

$$t_j := j\Delta t, \qquad j = 0, \ldots, n_t, \qquad \Delta t := \frac{1}{n_t},$$

as an equidistant grid for the discretization of the time interval $[0,1]$ (i.e., one model year). For time instant t_j, $j \in \{0, \ldots, n_t - 1\}$, vector $\mathbf{y}_{ji} \approx (y_i(t_j, x_k))_{k=1}^{n_x} \in \mathbb{R}^{n_x}$, firstly, represents the numerical approximation of a spatially discrete tracer y_i, $i \in \{1, \ldots, n_x\}$, and $\mathbf{q}_{ji} \approx (q_i(x_k, t_j, \mathbf{y_j}, \mathbf{u}))_{k=1}^{n_x} \in \mathbb{R}^{n_x}$, $\mathbf{u} \in \mathbb{R}^{n_u}$, the spatially discretized biogeochemical term q_i for the tracer y_i. Using a reasonable concatenation, $\mathbf{y}_j := (\mathbf{y}_{ji})_{i=1}^{n_y} \in \mathbb{R}^{n_y n_x}$ and $\mathbf{q}_j := (\mathbf{q}_{ji})_{i=1}^{n_y} \in \mathbb{R}^{n_y n_x}$, secondly, combine the numerical approximations as well as the biogeochemical terms of all tracers at time instant t_j. With an explicit discretization of the advection and horizontal diffusion as well as an implicit discretization of the vertical diffusion, the application of a semi-discrete Euler scheme for (1) results in a time-stepping

$$\mathbf{y}_{j+1} = \left(\mathbf{I} + \Delta t \mathbf{A}_j + \Delta t \mathbf{D}_j^h\right)\mathbf{y}_j + \Delta t \mathbf{D}_j^v \mathbf{y}_{j+1} + \Delta t \mathbf{q}_j(\mathbf{y}_j, \mathbf{u}), \qquad j = 0, \ldots, n_t - 1,$$

with the identity matrix $I \in \mathbb{R}^{n_x \times n_x}$ and the spatially discretized counterparts $\mathbf{A}_j, \mathbf{D}_j^h$ and $\mathbf{D}_j^v$ of the operators A, D_h and D_v at time instant t_j, $j \in \{0, \ldots, n_t - 1\}$. Defining the explicit and implicit transport matrices

$$\mathbf{T}_j^{\exp} := \mathbf{I} + \Delta t \mathbf{A}_j + \Delta t \mathbf{D}_j^h \in \mathbb{R}^{n_x \times n_x},$$
$$\mathbf{T}_j^{\mathrm{imp}} := \left(\mathbf{I} - \Delta t \mathbf{D}_j^v\right)^{-1} \in \mathbb{R}^{n_x \times n_x}$$

for each time instant t_j, $j \in \{0, \ldots, n_t - 1\}$, a time step of a marine ecosystem model simulation using the TMM is specified by

$$\mathbf{y}_{j+1} = \mathbf{T}_j^{\mathrm{imp}}\left(\mathbf{T}_j^{\exp}\mathbf{y}_j + \Delta t \mathbf{q}_j(\mathbf{y}_j, \mathbf{u})\right) =: \varphi_j(\mathbf{y}_j, \mathbf{u}), \qquad j = 0, \ldots, n_t - 1. \tag{9}$$

In practical computations, twelve sparse explicit and implicit transport matrices represent the monthly averaged tracer transport. These matrices are sparse because they are generated using a grid-point based ocean circulation model and the implicit ones (i.e., the inverse of the discretization matrices) include only the vertical part of the diffusion. For any time instant t_j, $j \in \{0, \ldots, n_t - 1\}$, the matrices are interpolated linearly. In the present paper, we used transport matrices computed with the MIT ocean model (Marshall et al. 1997) using a global configuration with a latitudinal and longitudinal resolution of 2.8125° and 15 vertical layers (see Khatiwala, Visbeck, and Cane 2005).

2.4 Computation of steady annual cycles

For a marine ecosystem model, an annual periodic solution (i.e., a steady annual cycle) is in a fully discrete setting a fixed-point of the nonlinear mapping

$$\Phi := \varphi_{n_t-1} \circ \ldots \circ \varphi_0$$

describing the time integration of (9) over one model year with φ_j, $j \in \{0, \ldots, n_t - 1\}$, defined in (9). Accordingly, an annual periodic solution fulfills

$$\mathbf{y}_{n_t} = \Phi(\mathbf{y}_0) = \mathbf{y}_0$$

applying the above iteration (9) over one model year. Starting from an arbitrary initial concentration vector $\mathbf{y}^0 \in \mathbb{R}^{n_y n_x}$ and using the fixed model parameters $\mathbf{u} \in \mathbb{R}^{n_u}$, a classical fixed-point iteration takes the form

$$\mathbf{y}^{\ell+1} = \Phi\left(\mathbf{y}^{\ell}, \mathbf{u}\right), \qquad \ell = 0, 1, \ldots. \tag{10}$$

If we interpret this fixed-point iteration (10) as pseudo-time stepping or *spin-up*, vector $\mathbf{y}^{\ell} \in \mathbb{R}^{n_y n_x}$ contains the tracer concentrations at the first time instant of model year $\ell \in \mathbb{N}$.

The difference between two consecutive iterates determined by

$$\varepsilon_\ell := \left\| \mathbf{y}^{\ell} - \mathbf{y}^{\ell-1} \right\|_2 \tag{11}$$

is a measure for the numerical convergence (i.e., the periodicity of the steady annual cycle) of the iteration (10) for model year $\ell \in \mathbb{N}$.

3 Initial concentrations

Each spin-up calculation starts with a given initial tracer concentration. The default initial concentration is a constant global mean tracer concentration where the nutrient tracer N is initialized with a global mean tracer concentration of $2.17\,\mathrm{mmol\,P\,m^{-3}}$ and the other tracers (i.e., the tracers DOP, P, Z and D) are initialized with a global mean tracer concentration of $0.0001\,\mathrm{mmol\,P\,m^{-3}}$.

We randomly generated initial tracer concentrations for each biogeochemical model. Based on continuous uniform, normal and lognormal distribution (e.g., Thomopoulos

2018), we created 100 different initial concentrations, respectively. For each tracer, the mean of the concentration matched the value of the default initial concentration in each box of the spatial discretization for every distribution, and all concentrations were non-negative. Apart from that, the partitioning of the mass between the tracers also corresponded to that of the default concentration, i.e., the major part of the mass belonged to the tracer N while the mass contribution of the other tracers in the overall mass was infinitesimal. The overall mass of each randomly generated initial concentration, in particular, coincided with the overall mass of the default concentration of the corresponding biogeochemical model. In addition to the three various distributions, we randomly created 100 initial concentrations for each biogeochemical model where the total concentration of a tracer was present in a single box of the spatial discretization, i.e., the concentration was zero in every box of the discretization except one single box containing the whole mass for this tracer. The box containing the whole mass for a tracer was randomly determined so that the boxes for the different tracers most likely differed. Analogous to the distributions above, the mass partitioning between the tracers resembled that of the default concentration.

We randomly varied the partitioning of the mass between the tracers for the generation of initial concentrations. Using the three distributions (uniform, normal and lognormal distribution) as well as using the concentration with the whole concentration in a single box of the discretization, we created 100 initial concentrations with respectively a random partitioning of the mass between the tracers for each biogeochemical model except for the N model with only one tracer. Moreover, we randomly generated 100 initial concentrations similar to the default initial concentration, where the tracer concentration of each tracer was globally constant, but the mass partitioning between the tracers was randomly determined. Lastly, we used constant initial concentrations with the same concentration for all tracers except for one tracer. More specifically, we gradually increased the tracer concentration by $0.1\,\mathrm{mmol\,P\,m^{-3}}$ starting from $0.0001\,\mathrm{mmol\,P\,m^{-3}}$ (except for one tracer) and, subsequently, reduced it for the remaining tracer (by number of tracers times $0.1\,\mathrm{mmol\,P\,m^{-3}}$) starting from $2.17\,\mathrm{mmol\,P\,m^{-3}}$.

In summary, we created 900 (and 400 for the N model) different initial concentrations and up to 42 by the stepwise concentration adjustment for each biogeochemical model.

4 Results

The spin-up calculation resulted almost in the same approximation of the steady annual cycle starting from different initial concentrations except for some outliers. In this section, we present the numerical results obtained for a wide variety of initial concentrations and assessed the accuracy of the calculated approximations.

4.1 Experimental setup

For the calculation of a steady annual cycle, we used the marine ecosystem toolkit for optimization and simulation in 3D (Metos3D) (Piwonski and Slawig 2016) and ran each spin-up over 10 000 model years. We applied the parameter vectors listed in Table 2

for the different biogeochemical models identifying the parameter vector of the N-DOP model with that of the MITgcm-PO4-DOP model.

We assessed the approximations of the steady annual cycle using different initial concentrations based on the norm of difference (11) and the accuracy of the approximation. For this purpose, we compared these approximations with a reference solution, denoted by $\mathbf{y}_{\text{default}}^{10000}$, namely the result obtained by a spin-up with Metos3D using the default initial concentration. We measured the accuracy of an approximation $\mathbf{x} \in \mathbb{R}^{n_y n_x}$ by the relative difference

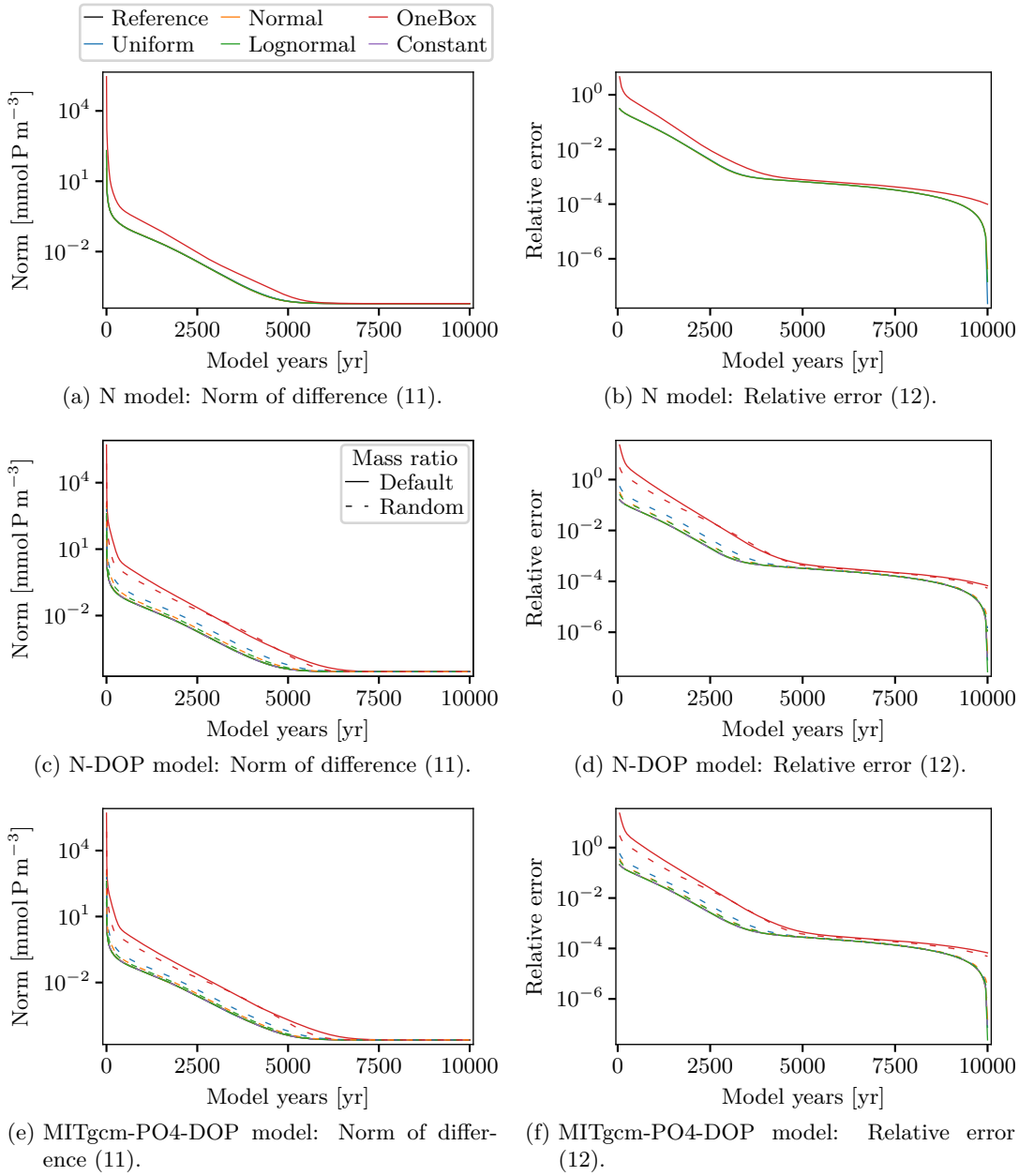
$$\frac{\left\|\mathbf{x} - \mathbf{y}_{\text{default}}^{10000}\right\|_2}{\left\|\mathbf{y}_{\text{default}}^{10000}\right\|_2} \tag{12}$$

and called this quantity (12) the *(relative) error* of the respective result $\mathbf{x}$.

4.2 Numerical Results

Regardless of the initial concentration, the spin-up calculation resulted in the same approximation of the steady annual cycle for the N, N-DOP and MITgcm-PO4-DOP model. Figure 1 demonstrates a similar convergence behavior for all different initial concentrations indicating that the spin-up reached nearly the same accuracy of the norm of differences (11). Particularly, the spin-up ended with the same approximation of the steady annual cycle for the different initial concentrations (Figure 1, right column). Using an initial concentration with the whole concentration in only one box of the discretization for each tracer, the spin-up required several thousand model years to distribute the tracer concentration throughout the ocean. Consequently, the norm of differences is slightly larger and the accuracy after 10 000 model years is slightly worse. To reach the accuracy of the other initial concentration types, further model years would be necessary. Furthermore, the marginal differences using a random partitioning of the mass (N-DOP and MITgcm-PO4-DOP model) resulted from the smaller concentration for the tracer N compared to the default initial concentration because most of the concentration was present as nutrients for the reference solution. Figure 2 shows the same results for all used initial concentrations. Except for the use of the initial concentration with the whole concentration in only one box of the spatial discretization for each tracer, the spin-ups reached almost the same norm of differences (11). More importantly, each of the spin-ups calculated an excellent approximation of the reference solution. Using the initial concentrations with the whole concentration in one single box for each tracer, the slightly larger relative error resulted from the required model years to distribute the tracer concentrations from the single boxes throughout the ocean. Nevertheless, these approximations adequately reflected the reference solution.

For the NP-DOP, NPZ-DOP and NPZD-DOP model, the initial concentration influenced the approximation of the steady annual cycle. The relative errors in Figure 3 indicate the spin-up calculation of nearly the same approximation of the steady annual cycle using the different initial concentrations for each of the three biogeochemical models except for some outliers with a huge relative error. Clearly, the norm of differences



(a) N model: Norm of difference (11).

(b) N model: Relative error (12).

(c) N-DOP model: Norm of difference (11).

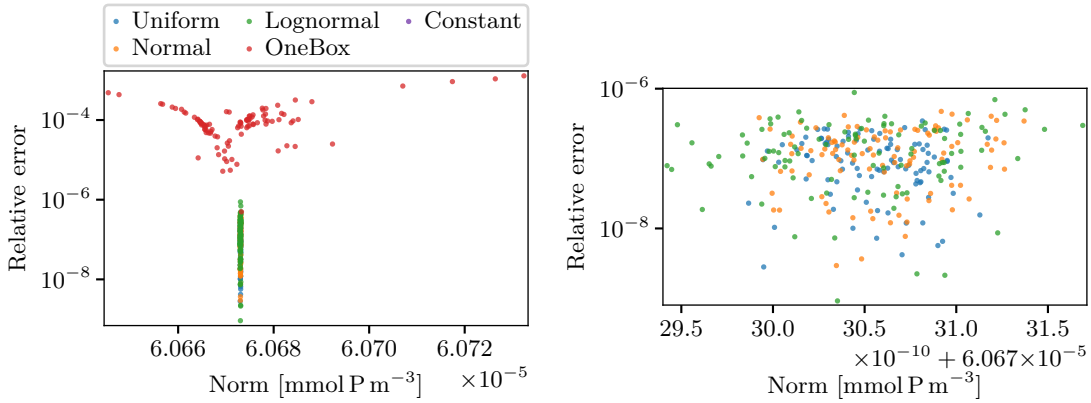
(d) N-DOP model: Relative error (12).

(e) MITgcm-PO4-DOP model: Norm of difference (11).

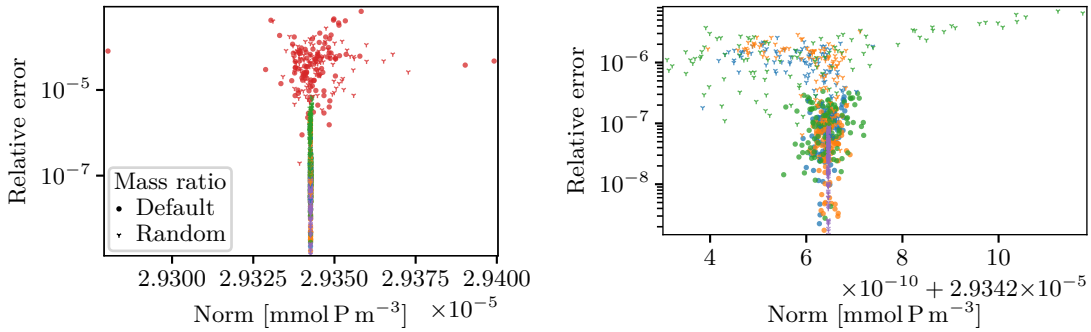
(f) MITgcm-PO4-DOP model: Relative error (12).

Figure 1: Convergence of the spin-up using different initial concentrations for the N, N-DOP and MITgcm-PO4-DOP model. Shown are the norm of difference (11) between consecutive iterations in the spin-up and the relative error (12) for one exemplary parameter vector of each initial concentration type.

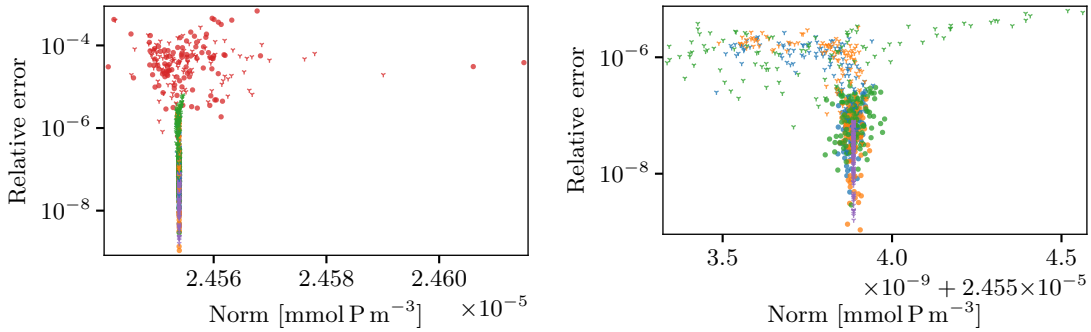
(11) was very small using the initial concentration that had been created with the log-normal distribution and random ratio of the tracer mass for the NP-DOP model as well as the initial concentration with the whole concentration in a single box for each tracer



(a) N model.



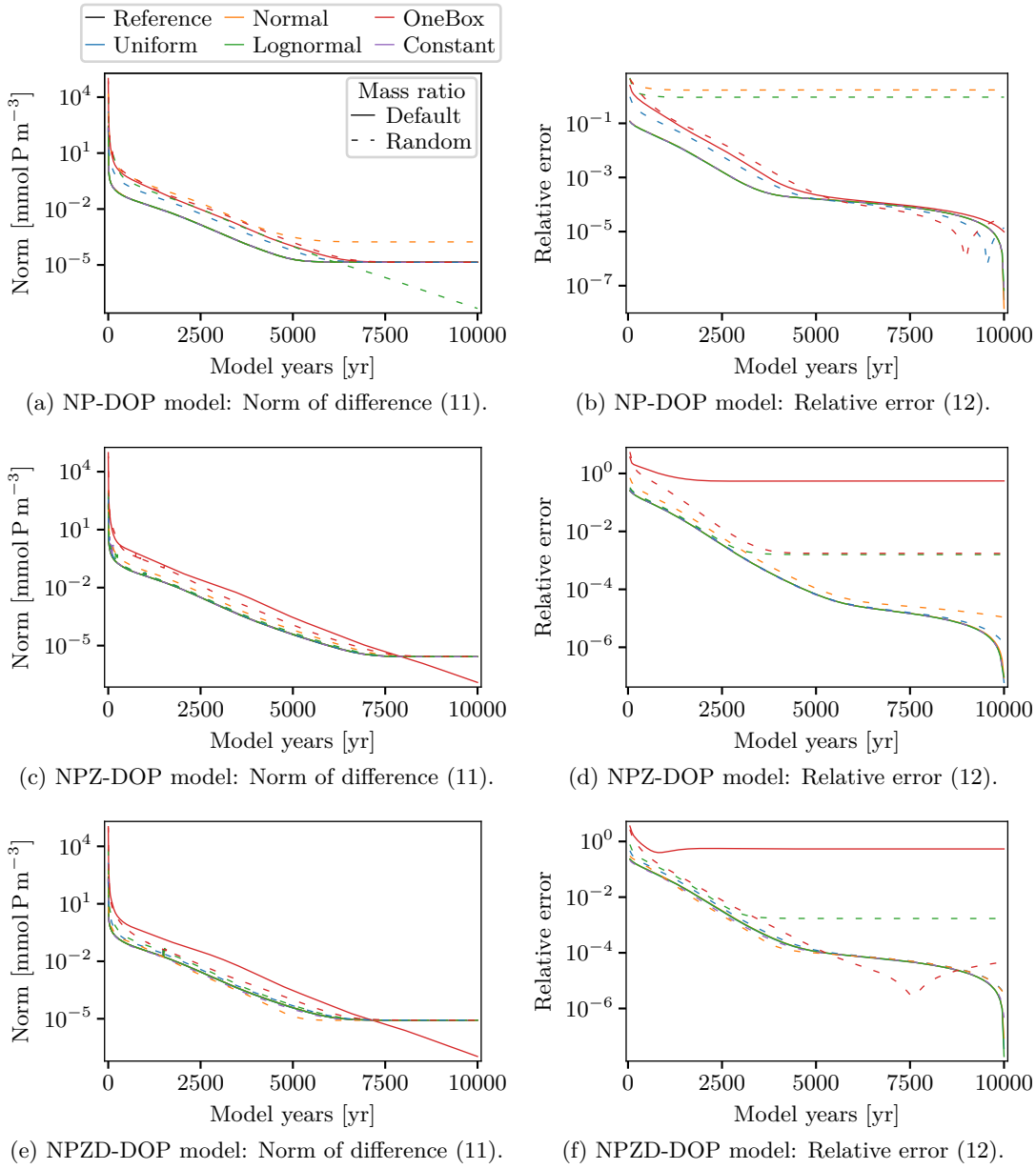
(b) N-DOP model.



(c) MITgcm-PO4-DOP model.

Figure 2: Visualization of the norm of difference (11) and the relative error (12) for $\ell = 10000$ for the N, N-DOP and MITgcm-PO4-DOP model. Shown are the results for 100 different initial concentrations respectively of the various initial concentrations types. The figures in the right column contain a detail of the figure in the left column.

for the NPZ-DOP and NPZD-DOP model. Still, the spin-up ended with an invalid approximation of the steady annual cycle (Figure 3). In these approximations, first, all tracers were nearly constant, second, the tracer N contained more mass than was ini-



(a) NP-DOP model: Norm of difference (11).

(b) NP-DOP model: Relative error (12).

(c) NPZ-DOP model: Norm of difference (11).

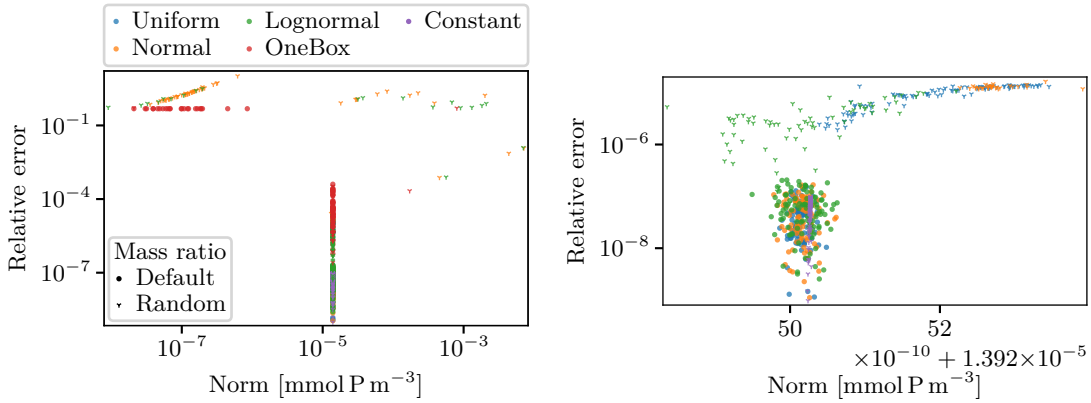
(d) NPZ-DOP model: Relative error (12).

(e) NPZD-DOP model: Norm of difference (11).

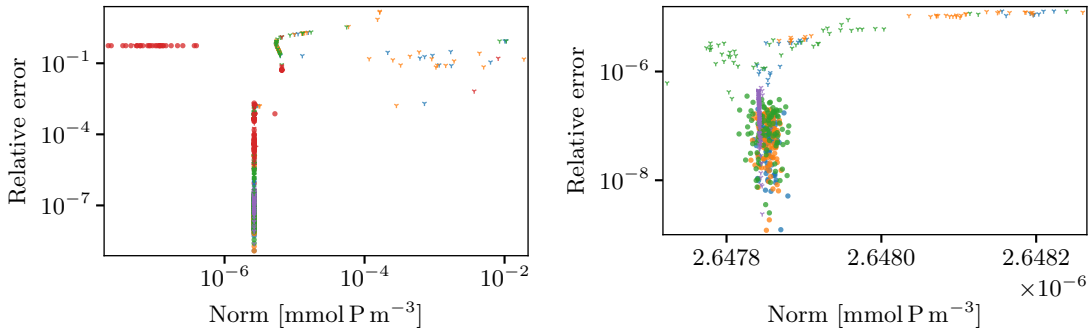
(f) NPZD-DOP model: Relative error (12).

Figure 3: Convergence of the spin-up using different initial concentrations for the NP-DOP, NPZ-DOP and NPZD-DOP model. Shown are the norm of difference (11) between consecutive iterations in the spin-up and the relative error (12) for one exemplary parameter vector of each initial concentration type.

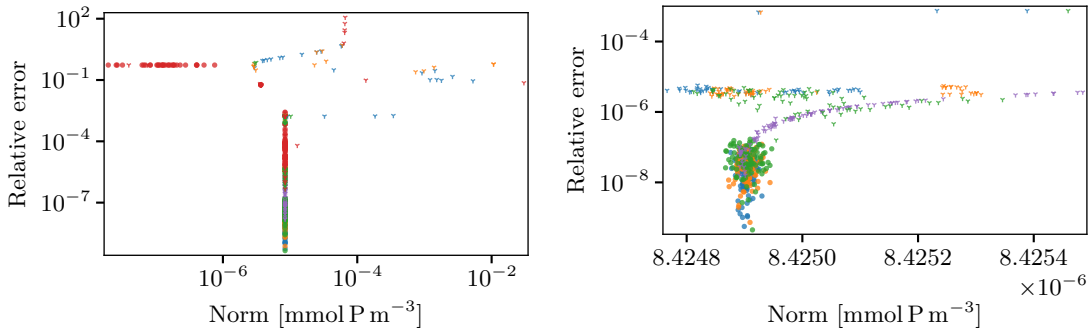
tially available and, third, the tracer concentrations of the other tracers (i.e., P, Z, D and DOP, if present) were exclusively negative. Likewise, the approximation computed with the initial concentration, which was generated with the normal distribution and random ratio of the tracer mass, was inadmissible because, as above, apart from the tracer N,



(a) NP-DOP model.



(b) NPZ-DOP model.



(c) NPZD-DOP model.

Figure 4: Visualization of the norm of difference (11) and the relative error (12) for $\ell = 10000$ for the NP-DOP, NPZ-DOP and NPZD-DOP model. Shown are the results for 100 different initial concentrations respectively of the various initial concentration types. The figures in the right column contain a detail of the figure in the left column.

all tracers were nearly constant and had exclusively negative concentrations (Figure 3). Conversely, the spin-up calculated a reasonable approximation of the reference solution for the NPZ-DOP and NPZD-DOP model starting from the initial concentration gener-

ated with the lognormal distribution and random ratio of the tracers (for the NPZ-DOP and NPZD-DOP model) or the initial concentration with the whole concentration in a single box and random ratio of the tracers (for the NPZ-DOP model), although the error (especially on the surface in the North Atlantic (Baffin Bay) or South Atlantic (southwest coast of Africa) for the tracers N and DOP) was slightly larger (Figure 3). Interestingly, the proportion of the tracer N compared to the other tracers was lowest of these three initial concentrations. Figure 4 summarizes the error of the approximations using the spin-up that was initialized with all different initial concentrations for the three different biogeochemical models NP-DOP, NPZ-DOP and NPZD-DOP. These approximations were mainly almost identical to the reference solution. As a result of the necessary distribution of the concentration throughout the ocean, the error was generally somewhat larger when an initial concentration with the whole concentration in single boxes was used. Especially in the case of using either a random ratio of the mass between the tracers or an initial concentration with the whole concentration in a single box for each tracer, there were, however, some initial concentrations for which the spin-up calculated inadmissible approximations containing negative tracer concentrations and, consequently, the error was large (Figure 4).

5 Conclusions

The existence of a unique steady annual cycle is important for the validation of marine ecosystem models. However, the theoretical analysis of the existence and uniqueness of a periodic solution is a challenging task for the different biogeochemical models (see e.g., Roschat and Slawig 2014; Roschat and Slawig 2015). In this study, we tested the uniqueness of a steady annual cycle by running a larger number of simulations starting from different initial concentrations for various biogeochemical models with increasing complexity. In addition to the default constant initial concentration used for simulating marine ecosystem models, we randomly generated a wide variety of different initial concentrations.

Starting from different initial concentrations, the numerical simulations finished with an almost identical approximation of a steady annual cycle, except for some outliers for the most complex models. On the one hand, the initial concentrations only marginally influenced the number of necessary model years to obtain the steady annual cycle of the reference solution. For the NP-DOP, NPZ-DOP and NPZD-DOP model, some initial concentrations, especially those with random partitioning of the tracer mass, led, on the other hand, to inadmissible steady annual cycles in which concentrations were negative.

The appearance of inadmissible steady annual cycles could be explained by a too large step size of the Euler method. A too large step size could lead to a draining of the biogeochemical model, which means the model could for instance require more nutrients in a time step than were available in a box of the discretization. Consequently, the concentration became negative. In fact, this process depended on both the model parameters and the tracer concentrations present in a box before the time step using the Euler method. Using an adequate time step, the transport matrix method and the

biogeochemical model did not generate negative concentrations because the equations of the biogeochemical model are quasi-positive (cf. Pierre 2010). Hence, one cause of the inadmissible steady annual cycles was a too large step size of the Euler method. Interestingly, the inadmissible approximations occurred, firstly, only for the three most complex biogeochemical models including quadratic terms (for the grazing function and model equations) and, secondly, for initial concentrations that had a random partitioning of tracer mass or the whole mass in a single box for each tracer. In particular, the use of the initial concentration using the whole mass in a box was unsuitable for the simulation in practice because several millennia were initially needed for the distribution of the tracer concentration throughout the ocean before the concentration approached the steady annual cycle, which explains why a spin-up over a larger number of model years was necessary (cf. Bernsen, Dijkstra, and Wubs 2008; Bryan 1984; Danabasoglu, McWilliams, and Large 1996). In brief, the inadmissible steady annual cycles resulted from numerical instabilities during the simulation and did not indicate the existence of two different steady annual cycles. Most notably, our numerical results suggested that the simulations finished always with the same steady annual cycle regardless of the initial concentration but this did not prove the existence and uniqueness of a periodic solution. Future work should, therefore, include the theoretical analysis of the existence and uniqueness of periodic solutions to marine ecosystem models.

In summary, the main points of this paper are the following:

- Regardless of the initial concentration, the spin-up calculation resulted in the same approximation for the N, N-DOP and MITgcm-PO4-DOP model.
- The initial concentration did not affect the approximation of the steady annual cycle for the NP-DOP, NPZ-DOP and NPZD-DOP model except for some outliers.
- For the NP-DOP, NPZ-DOP and NPZD-DOP model, the use of an initial concentration with a modified mass partitioning between the tracers could lead to an inadmissible approximation (occurrence of negative tracer concentrations).

Code and data availability

The code used to generate the data in this publication is available at `https://github.com/slawig/bgc-ann` and `https://metos3d.github.io/`. All used and generated data are available at `https://doi.org/10.5281/zenodo.5644701` (Pfeil and Slawig 2021).

References

Bacastow, Robert B. and Ernst Maier-Reimer (Apr. 1990). "Ocean-circulation model of the carbon cycle". In: *Climate Dynamics* 4.2, pp. 95–125. DOI: 10.1007/BF00208905.

– (1991). "Dissolved organic carbon in modeling oceanic new production". In: *Global Biogeochemical Cycles* 5.1, pp. 71–85. DOI: 10.1029/91GB00015.

Bernsen, Erik, Henk A. Dijkstra, and Fred W. Wubs (2008). "A method to reduce the spin-up time of ocean models". In: *Ocean Modelling* 20.4, pp. 380–392. DOI: 10.1016/j.ocemod.2007.10.008.

Bryan, Kirk (1984). "Accelerating the Convergence to Equilibrium of Ocean-Climate Models". In: *Journal of Physical Oceanography* 14.4, pp. 666–673. DOI: 10.1175/1520-0485(1984)014<0666:ATCTEO>2.0.CO;2.

Danabasoglu, Gokhan, James C. McWilliams, and William G. Large (1996). "Approach to Equilibrium in Accelerated Global Oceanic Models". In: *Journal of Climate* 9.5, pp. 1092–1110. DOI: 10.1175/1520-0442(1996)009<1092:ATEIAG>2.0.CO;2.

Dutkiewicz, Stephanie et al. (2005). *A three-dimensional ocean-seaice-carbon cycle model and its coupling to a two-dimensional atmospheric model: Uses in climate change studies*. Tech. rep. 122. Cambridge: MIT Joint Program on the Science and Policy of Global Change.

Fasham, Michael J. R., ed. (2003). *Ocean Biogeochemistry*. Global Change – The IGBP Series. Berlin et al.: Springer. DOI: 10.1007/978-3-642-55844-3.

Fennel, Katja et al. (2001). "Testing a marine ecosystem model: sensitivity analysis and parameter optimization". In: *Journal of Marine Systems* 28.1, pp. 45–63. DOI: 10.1016/S0924-7963(00)00083-X.

Fennel, Wolfgang and Thomas Neumann (2004). *Introduction to the Modelling of Marine Ecosystems*. Vol. 72. Elsevier Oceanography Series. Elsevier.

Ilyina, Tatiana et al. (2013). "Global ocean biogeochemistry model HAMOCC: Model architecture and performance as component of the MPI-Earth system model in different CMIP5 experimental realizations". In: *Journal of Advances in Modeling Earth Systems* 5.2, pp. 287–315. DOI: 10.1029/2012MS000178.

Keller, David P., Andreas Oschlies, and Michael Eby (2012). "A new marine ecosystem model for the University of Victoria Earth System Climate Model". In: *Geoscientific Model Development* 5.5, pp. 1195–1220. DOI: 10.5194/gmd-5-1195-2012.

Khatiwala, Samar (2007). "A computational framework for simulation of biogeochemical tracers in the ocean". In: *Global Biogeochemical Cycles* 21.3. DOI: 10.1029/2007GB002923.

Khatiwala, Samar, Martin Visbeck, and Mark A. Cane (2005). "Accelerated simulation of passive tracers in ocean circulation models". In: *Ocean Modelling* 9.1, pp. 51–69. DOI: 10.1016/j.ocemod.2004.04.002.

Kriest, Iris, Samar Khatiwala, and Andreas Oschlies (2010). "Towards an assessment of simple global marine biogeochemical models of different complexity". In: *Progress In Oceanography* 86.3-4, pp. 337–360. DOI: 10.1016/j.pocean.2010.05.002.

Le Quéré, Corinne et al. (2016). "Role of zooplankton dynamics for Southern Ocean phytoplankton biomass and global biogeochemical cycles". In: *Biogeosciences* 13.14, pp. 4111–4133. DOI: 10.5194/bg-13-4111-2016.

Marshall, John et al. (1997). "A finite-volume, incompressible Navier Stokes model for studies of the ocean on parallel computers". In: *Journal of Geophysical Research: Oceans* 102.C3, pp. 5753–5766. DOI: 10.1029/96JC02775.

Martin, John H. et al. (1987). "VERTEX: carbon cycling in the northeast Pacific". In: *Deep Sea Research Part A. Oceanographic Research Papers* 34.2, pp. 267–285. DOI: 10.1016/0198-0149(87)90086-0.

Oschlies, Andreas (2006). "On the use of data assimilation in biogeochemical modelling". In: *Ocean Weather Forecasting*. Ed. by E. P. Chassignet and J. Verron. Dordrecht: Springer, pp. 525–547. DOI: 10.1007/1-4020-4028-8_24.

Paltridge, Garth William and C. M. R. Platt (1976). *Radiative Processes in Meteorology and Climatology*. New York: Elsevier. DOI: 10.1002/qj.49710343713.

Parekh, P., Michael J. Follows, and Edward A. Boyle (2005). "Decoupling of iron and phosphate in the global ocean". In: *Global Biogeochemical Cycles* 19.2. DOI: 10.1029/2004GB002280.

Pfeil, Markus and Thomas Slawig (2021). *Unique steady annual cycle in marine ecosystem model simulations*. Version 1.0. Zenodo. DOI: 10.5281/zenodo.5644701.

Pierre, Michel (2010). "Global Existence in Reaction-Diffusion Systems with Control of Mass: a Survey". In: *Milan Journal of Mathematics* 78.2, pp. 417–455. DOI: 10.1007/s00032-010-0133-4.

Piwonski, Jaroslaw and Thomas Slawig (2016). "Metos3D: the Marine Ecosystem Toolkit for Optimization and Simulation in 3-D – Part 1: Simulation Package v0.3.2". In: *Geoscientific Model Development* 9.10, pp. 3729–3750. DOI: 10.5194/gmd-9-3729-2016.

Roschat, Christina and Thomas Slawig (2014). *Nontrivial Periodic Solutions of Marine Ecosystem Models of N-DOP type*. arXiv: 1409.7540 [math.AP].

– (2015). *Mathematical analysis of a marine ecosystem model with nonlinear coupling terms and non-local boundary conditions*. arXiv: 1403.4461 [math.AP].

Sarmiento, Jorge Louis and Nicolas Gruber (2006). *Ocean biogeochemical dynamics*. Princeton et al.: Princeton University Press.

Schartau, Markus and Andreas Oschlies (2003). "Simultaneous data-based optimization of a 1d-ecosystem model at three locations in the north Atlantic: Part I - method and parameter estimates". In: *Journal of Marine Research* 61.6, pp. 765–793. DOI: doi:10.1357/002224003322981147.

Schmittner, Andreas et al. (2005). "A global model of the marine ecosystem for long-term simulations: Sensitivity to ocean mixing, buoyancy forcing, particle sinking, and dissolved organic matter cycling". In: *Global Biogeochemical Cycles* 19.3. DOI: 10.1029/2004GB002283.

Thomopoulos, Nick T. (2018). *Probability distributions. With truncated, log and bivariate extensions*. Cham: Springer. DOI: 10.1007/978-3-319-76042-1.

Yool, Andrew, Ekaterina E. Popova, and Tom R. Anderson (2013). "MEDUSA-2.0: an intermediate complexity biogeochemical model of the marine carbon cycle for climate change and ocean acidification studies". In: *Geoscientific Model Development* 6.5, pp. 1767–1811. DOI: 10.5194/gmd-6-1767-2013.